SLAC-PUB-1431
(E/A)
May 1974

MUON SHIELDING AROUND HIGH ENERGY ELECTRON ACCELERATORS:

PART I. THEORY*

W. R. Nelson** and K. R. Kase+
Stanford Linear Accelerator Center
Stanford University, Stanford, California, U.S.A.

ABSTRACT

The production of muons from a high energy electron linac is calculated using the latest cross section theory. The shielding of these muons is calculated using the Fermi-Eyges multiple scattering formulation. The effect of various approximations in the calculations is discussed. A comparison is made between theory and experiment, and reasonable agreement is obtained in the forward direction. The experiment gives a significantly higher value for the absorbed dose, as compared to theory, for locations off the production axis. This is believed to be due to a background component in the total dose measured, and suggests the need for further experimentation with emphasis on fluence, as well as absorbed dose, measurements at distances far from the axis.

---

*Work supported by the U. S. Atomic Energy Commission.

**Submitted as partial fulfillment of the degree of Doctor of Philosophy at Stanford University.

+Present Address: Stanford University Medical School,
Stanford University,
Stanford, California 94305

(Submitted to Nucl. Instr. and Meth.)

1. Introduction

A high-energy, high-intensity electron linear accelerator, such as that presently being operated by the Stanford Linear Accelerator Center (SLAC), is capable of producing a high-intensity flux of muons by electromagnetic pair production. Serious problems can, at times, result from these muons since they quite easily penetrate rather massive shields.

In 1966 a series of theoretical and experimental investigations was undertaken to understand how to shield against muons produced by the Stanford two-mile accelerator (Nelson 1966a,b). The calculations did not agree with the experimental results (Nelson 1968), and since an independent analytical treatment by Alsmiller (1969) essentially showed agreement with the calculations by Nelson, a more elaborate experiment was performed. The results of that experiment are presented in the paper that follows this one, and we shall refer to that as Paper II.

The present study (referred to as Paper I) is a definite improvement over the theoretical treatment previously published (Nelson 1968, Alsmiller 1969) in that a more up-to-date expression for the coherent production of muons (i.e., from the nucleus as a whole) is used. Furthermore, the production of muons from individual nucleons (incoherent production) is included in this study, although only the elastic scattering contribution is presented because of mathematical difficulties. In all cases, the effect due to finite nuclear (nucleon) size--the form factor effect--is accounted for. The cross section theory is that of Tsai (1971) and Kim and Tsai (1972a,b, 1973).

We make use of the Alsmiller (1969, Alsmiller et al. 1968) formulation because of its generality and elegance of presentation, although it can be shown (Nelson 1973) that the original formulation of Nelson (1968) approaches that of Alsmiller for the small angles generally encountered in practice.

2. Muon Production Calculations

2.1. Differential Muon Fluence

The differential muon fluence that is produced when a high energy electron beam is completely attenuated in matter can be calculated by integrating the pair production cross section over the photon distribution in the electromagnetic cascade shower. This can be expressed by

$$d\Phi(E,\varphi;E_0)/dE = (2N_0X_0/AR^2)\int_{E+\mu}^{E_0-m} [d^2\sigma(k,E,\varphi)/d\Omega\, dE][d\ell/dk]dk$$

$$(cm^{-2} - GeV^{-1} - electron^{-1}) . \qquad (1)$$

In this equation, and in the equations that follow

φ is the production angle in laboratory coordinates (radians);

R is the distance from the target (cm);

E_0 is the total energy of the electron beam (GeV);

E is the total muon energy (GeV);

k is the energy of a photon in the shower (GeV);

m is the rest mass of the electron (0.000511 GeV);

μ is the rest mass of the muon (0.10566 GeV);

N_0 is Avogadro's number (6.022169×10^{23} mole^{-1});

X_0 is the radiation length of the target ($g - cm^{-2}$);

$d\ell/dk$ is the differential photon track length [which is the total path length throughout the shower traversed by photons in the increment dk at energy k (Rossi 1952)] ($r.l. - GeV^{-1} - electron^{-1}$); and

$\frac{d^2\sigma}{d\Omega\, dE}$ is the pair production cross section ($cm^2 - Gev^{-1} - sr^{-1}$).

The integration limits are determined by kinematics and the factor of two comes from the fact that we include both μ^+ and μ^-. A point source is assumed.

2.2. Differential Photon Track Length

In a previous paper (Nelson 1968) we have examined various expressions that can be used to describe the energy distribution of photons in the electromagnetic shower development. The formula that appears to be the best is one that has been derived by Clement (1963) and is given by

$$d\ell/dk = 0.964(u/k)[-\ln(1-u^2) + 0.686u^2 - 0.5u^4]^{-1} \quad (r.l. - GeV^{-1}), \qquad (2)$$

where u = fractional photon energy, k/E_0.

Alsmiller (1969) has used a Monte Carlo computer code by Zerby and Moran (1962a, 1962b, 1963) to calculate the differential photon track length for the specific case of 18 GeV electrons incident on a cylindrical copper target having a radius of 11.5 cm and a thickness of 24.5 cm. The Monte Carlo data are shown in figure 1 where a comparison is made with the Clement formula. The agreement is quite good

over the range 3 GeV to 10 GeV, but the Clement expression might be 10-20% too high in the region 10 GeV to 18 GeV, depending on the statistics of the Monte Carlo calculation. We will use the Clement formula for all of our muon fluence and absorbed dose calculations.

2.3. Muon Pair Production Cross Section

a.) Weizsacker-Williams Method of Kim and Tsai

Kim and Tasi (1972b, Tsai 1971) have derived (under the Born approximation) an expression for the energy-angle distribution of μ^+ (or μ^-) which is exact in the lowest order in α^3 (fine structure constant). This equation, which involves integrations with respect to the undetected muon and nucleus (or nucleon), requires rather tedious mathematical work and extensive computer programming to obtain cross section values. If we use this cross section formulation, together with the integral equations that will be presented in subsequent sections, the evaluation of the muon fluence on the downstream side of a shield becomes so difficult and time-consuming that it is impractical to do.

Recently, however, Kim and Tsai (1972a, 1973) have presented an improved Weizsacker-Williams method which, unlike the usual application of the Weizsacker-Williams method to the pair production problem (Gribov et al. 1962), takes form factors into account. Their result for the muon pair production cross section is summarized in the following equations:

$$d^2\sigma(k,E,\varphi)/d\Omega\, dE = (2\alpha^3/\pi k)(E^2/\mu^4)[(2x^2 - 2x+1)(1+L)^{-2} + 4x(1-x)\, L(1+L)^{-4}]\chi$$

$$(cm^2 - GeV^{-1} - sr^{-1}) , \qquad (3)$$

where

$$\chi = (1/2M_i) \int_{q^2_{min}}^{\mu^2(1+L)^2} q^{-4}\, dq^2 \int_{M_i^2}^{(u-\mu)^2} dM_f^2 [2q'^2_{min}\, W_1 + (q^2 - q^2_{min}) W_2], \quad (4)$$

and where

M_i = mass of target,

M_f = mass of final system,

x = E/k,

L = $(\varphi/\varphi_c)^2$,

φ_c = characteristic angle

= μ/E,

φ = laboratory angle of detected muon relative to the incident photon direction,

q^2 = four-vector momentum transfer (squared)

= $q \cdot q$,

q^2_{min} = $-2\,[\mu^2 - k\cdot p - E_{+s}(k_s - E_s) + p_{+s}p_{is}]$,

q'^2_{min} = $[k\cdot p/(k-E)]^2$,

p^2 = laboratory three-momentum of muon (squared)

= $E^2 - \mu^2$.

$k\cdot p$ = product of four-vector momenta

= $k(E - p\cos\varphi)$,

u^2 = $\mu^2 + M_i^2 + 2M_i(k-E) - 2k\cdot p$,

k_s = $(kM_i - k\cdot p)/u$,

E_{+s} = $(u^2 + \mu^2 - M_f^2)/2u$,

p^2_{+s} = $E^2_{+s} - \mu^2$,

$p_{is}^2 = M_i^2(k^2 + p^2 - 2pk \cos\varphi)/u^2$,

$E_s = (k\cdot p - \mu^2 + EM_i)/u$,

$\alpha = 1/137.03602$,

W_1, W_2 = form factors which appear in electron scattering from a nucleus (Drell and Walecka 1964).

Note: The notation $q\cdot q$ (or $k\cdot p$) specifically refers to taking the product of two four-vectors.

When the final hadronic system is a discrete state, as in the case of elastic scattering from a nucleus or a nucleon, the integration with respect to M_f^2 can be eliminated by using delta functions in W_1 and W_2. We will consider the cross section as having two contributions corresponding to whether the initial hadronic system is a nucleus or an individual nucleon. For the production from a nucleon the final state can be the same nucleon (elastic scattering) or can include meson production (inelastic scattering). The inelastic case, however, will not be included in this study because of the mathematical complexity involved (W_1 and W_2 cannot be represented by delta functions so that equation (4) is not easily obtained in analytic form). The significance of neglecting the inelastic scattering term will be discussed, along with other approximations, in later sections.

b.) Coherent Production of Muons

According to Kim and Tsai (1972b, Tsai 1971), as q_{min}^{-1} becomes comparable to the nuclear radius but not much smaller than the inter-nucleon distance ($R_0 = 1.2$ fermi), the most important form factors are the elastic form factors of the nucleus. This contribution is usually

referred to as coherent production because it is proportional to Z^2 (the nuclear charge acting as a whole). For muon pair production the effect of atomic electron screening is negligible and the nuclear form factors can be written in terms of the delta function, $\delta(M_f^2 - M_i^2)$ (Kim and Tsai 1972a, 1973)

$$W_1(\text{coh}) = 0, \tag{5}$$

$$W_2(\text{coh}) = 2M_i\ \delta(M_f^2 - M_i^2)Z^2(1 + q^2/r_N)^{-2}\ , \tag{6}$$

which, along with equations (3) and (4), give for the coherent cross section

$$(d^2\sigma/d\Omega\ dE)_{\text{coh}} = 2\alpha Z^2 r_0^2 (m/\mu)^2\ (E^2/\pi\varphi_c^2 k^3)(1+L)^{-2}$$

$$\times \{2(1-y)[1 - 2L(1+L)^{-2}] + y^2\} I_{\text{coh}}\ , \tag{7}$$

with

$$I_{\text{coh}} = \int_{q^2_{\min}}^{\mu^2(1+L)^2} q^{-2}\ dq^2(1 - q^2_{\min}/q^2)(1 + q^2/r_N)^{-2}\ , \tag{8}$$

where

$y = 1/x = k/E$,

$r_0 = 2.817939 \times 10^{-13}$ cm,

$r_N = 6(hc/2\pi)^2\ R_0^{-2}\ A^{-2/3}$ GeV^2 ,

$R_0 = 1.2 \times 10^{-13}$ cm,

$hc/2\pi = 1.9732891 \times 10^{-14}$ GeV - cm.

The integration can be performed analytically and the result is

$$I_{\text{coh}} = -2 + (1 + 2X_{\min})\ \ln[X_{\max}(1+X_{\min})/X_{\min}(1+X_{\max})]$$

$$+ (1-X_{\min}X_{\max})(1+X_{\max})^{-1} + (1+X_{\max})X_{\min}/X_{\max}\ , \tag{9}$$

where

$$X_{min} = q^2_{min}/r_N \ ,$$

$$X_{max} = \mu^2(1+L)^2/r_N \ .$$

c.) Incoherent Production of Muons

When q^{-1}_{min} is smaller than the internucleon distance, R_0, one must consider incoherent production in addition to the coherent production described by the above equations. In other words, for large values of q^2 the nucleons inside the nucleus act incoherently, and the cross section is proportional to the number of protons (or neutrons).

As we have stated earlier, we will only consider the elastic nucleon case---that is, meson production is excluded and $M_f^2 = M_i^2 = M_p^2$ (proton mass squared). This problem has been considered by Kim and Tsai (1972a, 1973), who give the following "quasi-elastic" form factors for a nucleus of charge Z and atomic mass A:

$$W_j(\text{inc}) = W_j(\text{quasi}) = P(q^2)[ZW^{el}_{jp} + (A-Z)\, W^{el}_{jn}] \ , \qquad (10)$$

where

W^{el}_{jp} = elastic proton form factor,

W^{el}_{jn} = elastic neutron form factor,

$P(q^2)$ = Pauli suppression factor,

and $j = 1,2$.

The Pauli suppression factor is due to the invocation of the exclusion principle, and essentially limits the final state of the nucleon to values not already occupied (Mcvoy and Van Hove 1962).

The function $P(q^2)$ can be derived (Kim and Tsai 1972b) by considering two Fermi spheres of radius p_F whose centers are displaced by Q. The fraction of the sphere volume that is non-intersecting is then $P(q^2)$. The result is

$$\begin{aligned} P(q^2) &= 1 && \text{when } Q \geq 2p_F , \\ &= 3Q[1 - (Q/p_F)^2/12]/4p_F && \text{when } Q < 2p_F , \end{aligned} \tag{11}$$

where

p_F = Fermi momentum = 0.250 GeV/c,

$$Q^2 = q^2[1 + q^2/4M_p^2] , \tag{12}$$

M_p = rest mass of the proton = 0.938259 GeV

= rest mass of neutron (approximately) .

For the elastic nucleon form factors, Kim and Tsai (1972a, 1972b, 1973) suggest using the following:

$$W_{1p}^{el} = 2M_p\, \delta(M_f^2 - M_p^2)\, G_{ep}^2 (2.79)^2\, \tau , \tag{13}$$

$$W_{2p}^{el} = 2M_p\, \delta(M_f^2 - M_p^2)\, G_{ep}^2 [1 + (2.79)^2\, \tau](1+\tau)^{-1} , \tag{14}$$

$$W_{1n}^{el} = 2M_p\, \delta(M_f^2 - M_p^2)\, G_{ep}^2 (1.91)^2\, \tau , \tag{15}$$

$$W_{2n}^{el} = 2M_p\, \delta(M_f^2 - M_p^2)\, G_{ep}^2 (1.91)^2\, \tau(1+\tau)^{-1} , \tag{16}$$

where

$$G_{ep} = (1+q^2/r_p)^{-2} ,$$

$r_p = 0.71$ GeV^2,

$\tau = q^2/4M_p^2$.

Exact calculations by Kim and Tsai (1972b) indicate that the contribution of the neutron terms to the incoherent cross section is small except at large production angles and for high momenta; whereas, the inelastic scattering component becomes quite significant under these conditions. Since we have ignored the inelastic contribution, it seems reasonable to exclude the neutron terms too, and we will assume that $W_{1n}^{el} = W_{2n}^{el} = 0$ in this study. We will take $W_{1p}^{el} = 0$ for the same reason (a discussion of this approximation will be given later). Therefore,

$$W_2(\text{inc}) = P(q^2) Z W_{2p}^{el} \quad , \tag{17}$$

$$W_1(\text{inc}) = 0 \quad . \tag{18}$$

Substituting into equations (3) and (4), we have

$$\begin{aligned} d^2\sigma/d\Omega\, dE)_{\text{inc}} &= d^2\sigma/d\Omega\, dE)_{2p} \\ &= 2\alpha Z r_0^2 (m/\mu)^2 \, (E^2/\pi\varphi_c^2 k^3)(1+L)^{-2} \\ &\quad \times \{2(1-y)\,[1 - 2L(1+L)^{-2}] + y^2\} I_{2p} , \end{aligned} \tag{19}$$

with

$$\begin{aligned} I_{2p} = \int_{q_{min}^2}^{\mu^2(1+L)^2} & q^{-2}\, dq^2 (1 - q_{min}^2/q^2)(1+q^2/r_p)^{-4} \\ & \times P(q^2)\,[1 + (2.79)^2\tau]\,(1+\tau)^{-1} \quad . \end{aligned} \tag{20}$$

Now, we make a further approximation (the significance of which will be discussed later)

$$q^2 \ll 4M_p^2 \qquad (\text{or} \quad \tau \ll 1) \quad ,$$

so that $(1 + \tau) \approx 1$ (and $Q^2 \approx q^2$). Then

$$I_{2p} = \int_{q^2_{min}}^{\mu^2(1+L)^2} q^{-2}\, dq^2 (1 - q^2_{min})(1 + q^2/r_p)^{-4} \times P(q^2)\,[1 + (2.79)^2\tau] \,. \qquad (21)$$

Equation (21) can be integrated exactly with the result

$$I_{2p} = 6\sqrt{r_p}\,[g_1(\xi_2) - g_1(\xi_1)] + [g_2(\zeta_2) - g_2(\zeta_1)] \,, \qquad (22)$$

where

$$g_1(\xi) = \rho_1/\xi + \rho_2 \tan^{-1}\xi + \xi[\rho_3/(1+\xi^2) + \rho_4/(1+\xi^2)^2 + \rho_5/(1+\xi^2)^3] \,, \qquad (23)$$

$$\rho_1 = x_{min} \,,$$
$$\rho_2 = (35x_{min} + 5c_1 + c_2 + c_3)/16,$$
$$\rho_3 = (19x_{min} + 5c_1 + c_2 + c_3)/16,$$
$$\rho_4 = (11x_{min} + 5c_1 + c_2 - 7c_3)/24,$$
$$\rho_5 = (x_{min} + c_1 - c_2 + c_3)/6,$$
$$c_1 = 1 - q^2_{min}[\tau - (4/3)],$$
$$c_2 = r_p[\tau(1 + 4q^2_{min}/3) - (4/3)],$$
$$c_3 = -4r_p^2\tau^2/3,$$
$$x_{min} = q^2_{min}/r_p,$$
$$\xi_1 = \sqrt{x_{min}} \,;$$
$$\xi_2 = (2\sqrt{r_p})^{-1} \,,$$

and

$$g_2(\zeta) = r_1\zeta^3/3 + r_2\zeta^2/2 + r_3\zeta + r_4 \ln\zeta - r_5/\zeta \,, \qquad (24)$$

$$\gamma_1 = (1 + x_{min})(1+ \tau r_p) ,$$

$$\gamma_2 = 3 + (4 - 3\tau r_p)x_{min} - 2\tau r_p,$$

$$\gamma_3 = -3 - 3x_{min}(2 - \tau r_p) + \tau r_p,$$

$$\gamma_4 = 1 + x_{min}(4 - \tau r_p),$$

$$\gamma_5 = -x_{min},$$

$$\zeta_1 = (1 + 4r_p)^{-1},$$

$$\zeta_2 = x_{max}/(1 + x_{max}) ,$$

$$x_{max} = \mu^2(1 + L)^2/r_p .$$

The total cross section is the sum of the coherent and incoherent cross sections.

2.4. Integral Muon Fluence and Absorbed Dose

The integral muon fluence and the absorbed dose are given, respectively, by

$$\Phi(E,\varphi;E_0) = \int_E^{E_0-m-\mu} [d\Phi/dE']dE' \quad (cm^{-2} - electron^{-1}), \tag{25}$$

and

$$D(E,\varphi;E_0) = \int_E^{E_0-m-\mu} f(E')[d\Phi/dE']dE' \quad (rad - electron^{-1}), \tag{26}$$

where $d\Phi/dE'$ is given by equation (1) and where the upper limit of integration is dictated by particle kinematics. The factor $f(E')$ converts particle fluence to absorbed dose. Generally, f is taken outside the integral as a constant such that 10 muons/cm^2/sec gives 1 mrad/hour (which is calculated by using a constant ionization loss of 1.75 MeV-cm^2/g) since the error involved in doing this is small. A more exact method is to consider f to be a function of energy according to the equation

$$f(E') = 1.602 \times 10^{-8} S_d(E') \qquad (\text{rad-cm}^2) , \qquad (27)$$

where $S_d(E')$ is the mass stopping power for muons traversing the detector medium with energy E'. Depending on the detector geometry and the secondary electron spectrum generated by the muons, a restricted mass stopping power might be required in order to obtain accurate results. Unrestricted, as well as restricted, stopping powers are discussed by Kase and Nelson (1972).

3. Muon Transport Through a Thick Shield

3.1. Muon Transport Using the Fermi-Eyges Scattering Theory: Alsmiller Formulation

Alsmiller et al. (1968) use the Eyges (1948) solution to the Fermi diffusion equation (Rossi and Greisen 1941) to obtain the muon current density as a function of depth and radius in a slab shield for the case of a monoenergetic muon emitted at an angle φ with respect to a normal to the slab face from a point source located at a distance (R-d) in front of the slab (see figure 2). Alsmiller (1969) then obtains the absorbed dose on the downstream side of the shield by

1) averaging the current density over all azimuthal angles of emission,
2) converting from current density to fluence (flux density in their terminology),
3) introducing the incident source distribution in energy and angle, and

4) using the fluence-to-absorbed dose conversion factor given by equation (27) above.

Their result is

$$D'(\theta;d,E_0) = \int_0^{\infty} \sin\varphi \, d\varphi \int_{E_m}^{E_0-m-\mu} [d\Phi(E,\varphi;E_0)/dE] \times C(T,\varphi;d)\, I_0[C(T,\varphi;d) \tan\theta \sin\varphi \cos\varphi] \times \{-C(T,\varphi;d)[\sin^2\varphi + \tan^2\theta \cos^2\varphi]\}\, f(T_d)\, dE \quad (\text{rad-electron}^{-1}) , \tag{28}$$

where

$$C(T,\varphi;d) = R^2/2A_2(T,\varphi;d) , \tag{29}$$

$$A_2(T,\varphi;d) = (\pi m^2/\alpha X_0) \int_0^{d/\cos\varphi} [(d/\cos\varphi) - z]^2 \times [T'(T' + 2\mu)/(T' + \mu)]^{-2}\, dz \quad (cm^2) , \tag{30}$$

$d\Phi(E,\varphi;E_0)/dE$ is defined by equation (1),

I_0 = zero order Bessel function of the first kind,

$f(T_d)$ is defined by equation (27),

and

$T = E - \mu$.

Also

1) $T' = E' - \mu$ is determined from the equation

$$\int_{T'}^{T} dT''/S(T'') = z = \eta(T) - \eta(T') , \tag{31}$$

where

$\eta(T)$ = range in the shield for a muon of kinetic energy T (under the continuous slowing-down approximation)

$$= \int_0^T dT''/S(T'') \quad (\text{cm}) ,$$

$S(T'')$ = total stopping power (GeV/cm) for the shield at kinetic energy T'' (includes ionization (unrestricted), radiation, pair production, and nuclear interaction losses);

2) T_d is the kinetic energy of a muon at the detector location and is obtained from the equation

$$\int_{T_d}^{T} dT''/S(T'') = d/\cos\varphi = \eta(T) - \eta(T_d); \tag{32}$$

3) $E_m = T_m + \mu$ where T_m is the kinetic energy of a muon that just gets through the shield to the detector, defined according to the equation

$$\int_0^{T_m} dT''/S(T'') = d/\cos\varphi = \eta(T_m) . \tag{33}$$

Now, we can obtain the integral muon fluence by letting $f(T_d) = 1$ in equation (28), that is,

$$\Phi'(\theta;d,E_0) = D'(\theta;d,E_0)\Big|_{f=1} . \tag{34}$$

If we now make the small angle approximation

$$\sin\varphi \approx \varphi,$$

$$\cos\varphi \approx 1,$$

$$\tan\theta \approx \theta$$

in equation (28), we obtain a result derived earlier by Nelson (1968). We will use equations (28) through (34), along with the cross sections presented above, for the calculations that follow.

3.2. Range versus Energy

A set of range-energy curves for muons in various materials is provided in figure 3. The curves represent our extension of previous calculations (Barkas and Berger 1964) to higher energies, and includes pair production, bremsstrahlung, and nuclear interaction losses (Hayman et al. 1963). This was done in a manner similar to that by Thomas (1964). The earth curve was scaled (by density) from the aluminum curve.

4. A Discussion on the Approximations

4.1. Coherent versus Incoherent (Elastic and Inelastic) Contributions

In Section 2.3 we arrived at an analytical expression for the incoherent (elastic) proton pair production cross section (equations (19) through (24)) by assuming that $W_{1p}^{el} = 0$ and by making the approximation

$$q^2 \ll 4M_p^2 ,$$

which allowed us to take

$$(1 + q^2/4M_p^2) \approx 1,$$

and

$$Q^2 = q^2[1 + q^2/4M_p^2] \approx q^2 .$$

Accordingly, the elastic proton contribution to the total muon fluence for various detector angles is given in Table 1. The shield material and thickness, as well as the source-to-detector distance, that were used to determine Table 1 (and several other tables to follow) correspond to an experimental situation described in Paper II. We see that the addition of the elastic proton component amounts to less than 10% for angles smaller than 120 milliradians. As the detector angle increases past 120 milliradians, the W_{2p} term adds substantially to the coherent fluence, and accounts for about 40% of the total at 150 milliradians.

The effect of the approximation, $q^2 \ll 4M_p^2$, as well as the addition of the W_{2n} term, can be seen by numerically integrating the cross section formulas defined in Section 2.3. Tables 2a and 2b give the various contributions for an 18 GeV photon incident on a copper target producing muons having total energies of 8 and 16 GeV, respectively. As expected, the coherent term dominates in the forward direction (this was apparent in Table 1 also). At large production angles the elastic proton term (W_{2p}) becomes comparable to, and eventually dominates over, the coherent component. The elastic neutron term (W_{2n}) is observed to be much less important. The approximation, $q^2 \ll 4M_p^2$, causes the W_{2p} term to be overestimated at large angles (about 8% at 150 milliradians). Interestingly, the approximation helps to compensate for the fact that we took W_{2n} equal to zero in our calculations of the muon fluence.

The W_{1p} and W_{1n} terms were not included in our calculations either. This is justified by the fact that whenever W_{1p} and W_{1n} (and W_{2n}, for that matter) are significant, then so is the inelastic

nucleon term. We are unable, in this study to account for the inelastic contribution due to lack of an analytical expression for the cross section. Recalling the basic cross section formula under the Weizsacker-Williams approximation (equation (4)), we see that the difficulty arises because we cannot represent the final state as a delta function (of the mass squared) since it is broken up into a number of particles (meson production).

The inelastic proton cross section for the pair production of muons can be obtained by performing an exact (Born) calculation numerically. This has been done by Kim and Tsai (1972b), and, as you will recall (Section 2.3), the calculation requires extensive computer time, making it prohibitive to include it in equation (1). The effect in beryllium can be seen in Table 3, which is taken from the paper by Kim and Tsai (1972b). The column labeled "Be Quasi-Elastic" is defined according to equation (10). As usual, the coherent production dominates at zero degrees. At 99.0 milliradians the quasi-elastic contribution, which contains W_{1p}^{el}, W_{2p}^{el}, W_{1n}^{el}, and W_{2n}^{el} terms, is ten times the coherent component. Furthermore, the proton elastic (W_{1p}^{el}, W_{2p}^{el}) and inelastic terms are comparable to one another at this angle. It is apparent, therefore, that the elastic and inelastic terms become significant at large production angles, corresponding to large momentum transfers, and it may not be correct to keep one component and to neglect the others. We will attempt to estimate the net effect in Section 4.2 when we compare the Weizsacker-Williams cross section directly with the exact (Born) calculation, both by Kim and Tsai (1972a, 1973, 1972b)

The following conclusions are reached in this section:

1) the elastic neutron contributions, described by W_{2n}, and to a much lesser extent, W_{1n}, are not very significant, so that we can take $W_{1n} = W_{2n} = 0$ without too much effect;

2) the approximation, $q^2 \ll 4M_p^2$, is of minor significance (less than 8% effect), and is in the direction that overestimates the cross section. If anything, it compensates for making the approximation, $W_{2n} = 0$;

3) the W_{2p} contribution is not important in the muon fluence (absorbed dose) estimates for angles less than 120 milliradians. At detector angles greater than 120 milliradians, the elastic proton contribution from W_{2p} becomes significant (about 40%);

4) the W_{1p} contribution has not been specifically looked at, but if it is important so will be the inelastic nuclear effects.

4.2. Comparison of the Weizsacker-Williams and the Exact (Born) Cross Sections (Elastic Only)

In this section we compare the Weizsacker-Williams approximation of the differential muon pair production cross section with the more exact (Born) method, both due to Kim and Tsai (1972a, 1973, 1972b). The Born-data were obtained by using Tsai's computer code, slightly modified by us to treat the present problem. Figure 4 plots both cross sections for 18 GeV photons incident on a copper target. Two muon energies, 8 and 16 GeV, are shown. A comparison is made between the coherent term alone and the coherent and incoherent (elastic) components

added together. All of the elastic form factors ($W_1(coh)$, $W_2(coh)$, W_{1p}^{el}, W_{2p}^{el}, W_{1n}^{el}, and W_{2n}^{el}) are used in the Born calculation; whereas, the Weizsacker-Williams estimate plotted in figure 4 only uses $W_2(coh)$ and W_{2p}^{el}. Furthermore, the approximation, $q^2 \ll 4M_p^2$, is made in this version of W.W.

At small angles and for muon energies that are not close to the incident photon energy, the agreement between the W.W. and the Born cross sections is reasonably good. This corresponds to small momentum transfers. As q^2 gets larger, the difference gets bigger, as can be seen in the region near 80 milliradians for the $E = 16$ GeV curves. At this angle, the total Born curve is 33 times higher than the coherent W.W. for $E = 16$ GeV, but only 32% higher for $E = 8$ GeV. It should be pointed out that the elastic incoherent contribution vanishes at some point due to kinematic limitations (e.g., at 120 milliradians on the $E = 16$ GeV curves).

Although the difference between the exact and W.W. cross sections is substantial in some regions, particularly when E is near k, the net effect is relatively insignificant in the calculation of the multiple scattered muon fluence (or absorbed dose). This can be understood from the fact that the production of the lower energy muons is more probable. For example, the $E = 8$ GeV cross section is two to three orders of magnitude higher than the $E = 16$ GeV one, as is apparent in figure 4. To observe the effect directly, we need only re-examine Table 1, which gives the percent increase in the muon fluence as a result of adding the W_{2p} component to the coherent component. Table 1 corresponds to the solid lines in figure 4. The largest increase in Table 1 is about 40%.

The most we can expect from an exact (Born) calculation (according to figure 4) would be about twice this, or 80%. Furthermore, the inelastic production, as indicated in Table 3, cannot contribute too much more. All in all, an increase of 100% over the coherent W.W. calculation of the muon fluence or the absorbed dose might be reasonable at large angles (say, 130-150 milliradians).

5. Comparison of Present Theory with Previous Calculations and with Experiment

A comparison has been made in figure 5 between the present method of calculating the transport of muons through a shield with that of Nelson (1968), and with Alsmiller (1969). In order to make this comparison, the old cross section formula of Tsai (1971) (see equation (6) of Nelson (1968)) was used. The calculations were based on the following data: E_0 = 18.0 GeV, P = 16.2 kW, t = 258 min, R = 519 cm, d = 427 cm. The unrestricted stopping power for ^{7}LiF was used.

The calculation by Nelson (1968) made use of an approximate form for A_2. Whereas, the present formulation (see Section 3) is precisely the same as that of Alsmiller (1969), and we now have agreement at small angles and a slight disagreement (20%) at the larger angles.

In Figure 6, we compare the present study with the experimental data of Nelson (1968), where we now use the latest cross section formulae (coherent production only) and the restricted stopping power for ^{7}LiF (the energy cutoff for the detector geometry used in the experiment was estimated to be 0.8 MeV). It is quite apparent that the present method of calculation is much better at small angles. At zero milliradians

the new cross section accounts for a 39% decrease in the calculated absorbed dose, and the use of a restricted in place of an unrestricted stopping power accounts for a further decrease of 22%. At 70 milliradians the corresponding decreases are 67% and 13%, respectively. In addition, as we have seen in figure 5, the present transport theory formulation increases the absorbed dose from that calculated by Nelson (1968) by 47% at 70 milliradians, and makes no difference at zero milliradians.

The agreement between the present theory and the experiment by Nelson (1968) now appears to be reasonable at small angles. As the detector angle increases, however, the experimental points are more than a factor of three higher than the calculation. As we shall see in the paper following this one (Paper II), this discrepancy can be accounted for, in part, by a photon background contribution to the total absorbed dose measured by the LiF detector. Only a very small part can be accounted by the approximations in the cross section theory, as discussed in Section 4.

Two additional comments are in order at this point. First, as we have indicated in Section 4, the coherent contribution should account for most of the muon dose. Our calculations indicate, in fact, that inclusion of the incoherent-proton contribution accounts for less than a 2% increase of the dose in figure 6. Second, if we allow the nuclear form factor to approach unity (thereby reducing the nucleus to a point), the present does calculation reduces to the dose calculation using the old cross section, as expected.

6. Conclusions

The present method of calculation is far superior to the original calculation of Nelson (1968). The more general transport formulation of Alsmiller (1969) and more reliable muon production cross sections are used. Coherent production--that is, production of muon pairs whereby the nucleus acts as a whole--is the dominant source. For the calculation of absorbed dose, it appears as if one should use a restricted rather than an unrestricted stopping power. This depends, of course, on the detector system used in the measurement.

Comparison of absorbed dose calculation and measurement is reasonably good at small detector angles. At large angles the absorbed dose measurement is much higher than theory allows, even considering the approximations in the cross section theory. In an attempt to resolve this disagreement, the experiment described in the paper following this one (Paper II) was performed.

ACKNOWLEDGMENTS

The authors are grateful for the many discussions with Drs. R. C. McCall, H. DeStaebler, Jr., R. Mozley, B. Richter, A. Leonard, W. Swanson, L. Keller, Y. Tsai, and J. Lord (University of Washington).

TABLE 1

COMPARISON OF THE COHERENT MUON FLUENCE WITH THE INCOHERENT (ELASTIC PROTON, W_{2p} ONLY) MUON FLUENCE FOR GAP A*+

DETECTOR ANGLE, θ (mradians)	COHERENT FLUENCE (cm^{-2}-$Coul^{-1}$)	INCOHERENT FLUENCE (cm^{-2}-$Coul^{-1}$)	(INCOHERENT/COHERENT)%
0	2.155×10^{10}	0.024×10^{10}	1.1
10	1.811×10^{10}	0.020×10^{10}	1.1
20	1.133×10^{10}	0.014×10^{10}	1.2
30	5.941×10^{9}	0.080×10^{9}	1.3
40	2.856×10^{9}	0.042×10^{9}	1.5
50	1.310×10^{9}	0.025×10^{9}	1.9
60	5.793×10^{8}	0.107×10^{8}	1.8
70	2.446×10^{8}	0.061×10^{8}	2.4
80	9.901×10^{7}	0.239×10^{7}	2.4
90	3.814×10^{7}	0.116×10^{7}	3.1
100	1.397×10^{7}	0.055×10^{7}	3.9
110	4.876×10^{6}	0.262×10^{6}	5.4
120	1.630×10^{6}	0.142×10^{6}	8.7
130	5.270×10^{5}	0.753×10^{5}	14.3
140	1.684×10^{5}	0.395×10^{5}	23.4
150	5.398×10^{4}	2.138×10^{4}	39.6

*Gap A refers to a typical experimental situation described in Paper II (following this paper), where: R = 555.19 cm and d = 509.91 cm (iron).

+With the approximation, $q^2 \ll 4M_p^2$ (see Section 2.3).

Note: W_{2p} is really a "quasi-elastic" incoherent form factor defined by equation (10) in the text.

TABLE 2a

DIFFERENTIAL MUON PAIR PRODUCTION CROSS SECTION FOR COPPER:

ELASTIC CONTRIBUTIONS USING THE WEIZSACKER-WILLIAMS APPROXIMATION (k = 18 GeV, E = 8 GeV)

PRODUCTION ANGLE, φ (mradians)	W_2(coh)	W_{2p} (millibarns/GeV-steradian)	W_{2p}, W_{2n} (millibarns/GeV-steradian)	W_{2p}* (millibarns/GeV-steradian)
0	7.726×10^{0}	2.451×10^{-2}	2.462×10^{-2}	2.454×10^{-2}
10	4.000×10^{0}	2.202×10^{-2}	2.226×10^{-2}	2.208×10^{-2}
30	1.250×10^{-1}	2.974×10^{-3}	3.197×10^{-3}	3.046×10^{-3}
50	8.878×10^{-3}	4.311×10^{-4}	4.735×10^{-4}	4.481×10^{-4}
70	1.063×10^{-3}	1.044×10^{-4}	1.156×10^{-4}	1.094×10^{-4}
100	6.641×10^{-5}	2.067×10^{-5}	2.324×10^{-5}	2.175×10^{-5}
130	5.595×10^{-6}	5.412×10^{-6}	6.227×10^{-6}	5.764×10^{-6}
150	1.261×10^{-6}	2.356×10^{-6}	2.764×10^{-6}	2.540×10^{-6}

*With the approximation, $q^2 \ll 4M_p^2$ (see Section 2.3)

Note: W_{2p} and W_{2n} are really "quasi-elastic" incoherent form factors, defined by equation (10).

TABLE 2b

DIFFERENTIAL MUON PAIR PRODUCTION CROSS SECTION FOR COPPER:

ELASTIC CONTRIBUTIONS USING THE WEIZSACKER-WILLIAMS APPROXIMATION (k = 18 GeV, E = 16 GeV)

PRODUCTION ANGLE, φ (mradians)	W_2(coh)	W_{2p}	W_{2p}, W_{2n}	W_{2p}^*
		(millibarns/GeV-steradian)		
0	3.548×10^{1}	1.498×10^{-1}	1.504×10^{-1}	1.499×10^{-1}
10	2.011×10^{0}	4.214×10^{-2}	4.381×10^{-2}	4.258×10^{-2}
30	3.707×10^{-3}	9.744×10^{-4}	1.093×10^{-3}	1.024×10^{-3}
50	2.964×10^{-5}	6.690×10^{-5}	7.906×10^{-5}	7.244×10^{-5}
70	7.718×10^{-7}	4.931×10^{-6}	6.330×10^{-6}	5.754×10^{-6}
100	1.511×10^{-8}	3.070×10^{-8}	4.482×10^{-8}	5.204×10^{-8}
130	8.844×10^{-10}	0	0	0
150	1.946×10^{-10}	0	0	0

*With the approximation, $q^2 \ll 4M_p^2$ (see Section 2.3)

Note 1: W_{2p} and W_{2n} are really "quasi-elastic" incoherent form factors, defined by equation (10).

Note 2: The zeros indicate that the cross section vanishes because of kinematics.

TABLE 3

DIFFERENTIAL MUON PAIR PRODUCTION CROSS SECTION FOR BERYLLIUM:
ELASTIC AND INELASTIC CONTRIBUTIONS USING THE BORN APPROXIMATION (k = 20 GeV, E = 16 GeV)*

PRODUCTION ANGLE (mradians)	BE COHERENT	PROTON ELASTIC	NEUTRON ELASTIC	BE QUASI-ELASTIC	PROTON INELASTIC
		(millibarns/GeV-steradian)			
0	7.145×10^{-1}	5.014×10^{-2}	2.486×10^{-4}	2.480×10^{-2}	1.210×10^{-3}
26.4	8.428×10^{-4}	1.287×10^{-4}	7.248×10^{-6}	3.141×10^{-4}	3.541×10^{-5}
46.2	2.538×10^{-5}	8.195×10^{-6}	1.029×10^{-6}	2.982×10^{-5}	4.993×10^{-6}
66.1	1.438×10^{-6}	9.955×10^{-7}	2.026×10^{-7}	4.523×10^{-6}	8.870×10^{-7}
99.0	2.977×10^{-8}	4.697×10^{-8}	1.570×10^{-8}	2.664×10^{-7}	4.466×10^{-8}
132.2	1.610×10^{-9}	9.891×10^{-10}	4.032×10^{-10}	5.972×10^{-9}	4.747×10^{-10}

*Taken from Table II of Kim and Tsai (1972b).

REFERENCES

R. G. Alsmiller, Jr., M. Leimdorfer, and J. Barish, High-energy muon transport and the muon backstop for a 200-GeV proton accelerator. Oak Ridge National Laboratory Report Number ORNL-4322, Oak Ridge, Tennessee (1968).

R. G. Alsmiller, Jr., High-energy (< 18 GeV) muon transport calculations and comparison with experiment, Nucl. Instr. Meth. 71 (1969), 121.

W. H. Barkas and M.J. Berger, Tables of energy losses and ranges of heavy charged particles, National Aeronautics Space Administration Report Number NASA-SP-3013 (1964).

G. Clement, Parcours differentiel des photons produits par un électron de tréshaute énergie dons une cible épaisse, Comptes Rendus 257 (1963) 2971; translated from the French for the Stanford Linear Accelerator Center, SLAC-TRANS-141, Stanford University, Stanford, California (February 1972).

S. D. Drell and J. D. Walecka, Electrodynamic processes with nuclear targets, Ann. Phy. 28 (1964), 18.

L. Eyges, Multiple scattering with energy loss, Phys. Rev. 74 (1948), 1534.

V. N. Gribov, V. A. Kolkunov, L.B. Okun', and V. M. Shekhter, Covariant derivation of the Weizsacker-Williams formula, Sov. Phy. JETP 14 (1962), 1308.

P. J. Hayman, N. S. Palmer and A. W. Wolfendale, The rate of energy loss of high-energy cosmic ray muons, Proc. Roy. Soc. A275 (1963), 391.

K. R. Kase, and W. R. Nelson, Concepts of radiation dosimetry, Stanford Linear Accelerator Center Report Number SLAC-153, Stanford University, Stanford, California (1972).

K. J. Kim and Y. S. Tsai, An improved Weizsacker-Williams method and photoproduction of lepton pairs, Phys. Lett. 40B (1972a), 662.

K. J. Kim and Y. S. Tsai, Photoproduction of electrons, muons and heavy leptons, Stanford Linear Accelerator Center Report Number SLAC-PUB-1105, Stanford University, Stanford, California (1972b).

K. J. Kim and Y. S. Tsai, Improved Weizsacker-Williams method and its application to lepton and W-boson pair production, Stanford Linear Accelerator Center Report Number SLAC-PUB-1106 (Rev), Stanford University, Stanford, California (1973).

K. W. Mcvoy and L. Van Hove, Inelastic electron-nucleus scattering and nuclear-nuclear correlations, Phys. Rev. 125 (1962), 1034.

W. R. Nelson, Muon production calculations for muon shielding, Stanford Linear Accelerator Center Report Number SLAC-TN-66-37, Stanford University, Stanford, California (1966a).

W. R. Nelson, Multiple elastic scattering of muons with energy loss, Stanford Linear Accelerator Center Report Number SLAC-TN-66-41, Stanford University, Stanford, California (1966b).

W. R. Nelson, The shielding of muons around high-energy electron accelerators: theory and measurement, Nucl. Instr. Meth. 66 (1968), 293.

W. R. Nelson, The shielding of muons around high energy electron accelerators: theory and measurement, Ph.D. Thesis, Graduate Division Special Program, Stanford University, Stanford, California (1973).

B. Rossi, High-Energy Particles (Englewood Cliffs, New Jersey: Prentice-Hall (1952)).

B. Rossi and K. Greisen, Cosmic-ray theory, Rev. Mod. Phys. 13 (1941), 240.

R. H. Thomas, Energy loss of high-energy muons, Lawrence Berkeley Laboratory Report Number UCID-10010, University of California, Berkeley, California (1964).

Y. S. Tsai, Estimates of secondary-beam yields at SLAC, SLAC Users Handbook, C.3-1, Stanford Linear Accelerator Center, Stanford University, Stanford, California (1971).

C. D. Zerby and H. S. Moran, Studies of the longitudinal development of high-energy electron-photon cascade showers in copper, Oak Ridge National Laboratory Report Number ORNL-3329, Oak Ridge, Tennessee (1962a).

C. D. Zerby and H. S. Moran, A Monte Carlo calculation of the three-dimensional development of high-energy electron-photon cascade showers, Oak Ridge National Laboratory Report Number ORNL-TM-422, Oak Ridge, Tennessee (1962b).

C. D. Zerby and H. S. Moran, Studies of the longitudinal development of electron-photon cascade showers, J. Appl. Phy. 34 (1963), 2445.

FIGURES

Figure 1: Comparison of the Clement photon track length expression with Monte Carlo data.

Figure 2: a) Shielding diagram showing the source at T and the detector positions at P (unscattered) and P' (scattered).

b) Downstream plane of shield with relative positions of points O, P, and P' (looking towards the target).

Figure 3: Range-energy curves for muons in various materials.

Figure 4: Comparison of the Born and the Weizsacker-Williams cross sections for k = 18 GeV and for E = 8 GeV and E = 16 GeV (copper target).

Figure 5: Comparison of the Alsmiller and Nelson calculations with the present calculation--using the old photoproduction cross section (see equation (6) of (Nelson, 1968)), and the unrestricted stopping power (for ^{7}LiF).

Figure 6: Comparison of new and old calculations with experiment.

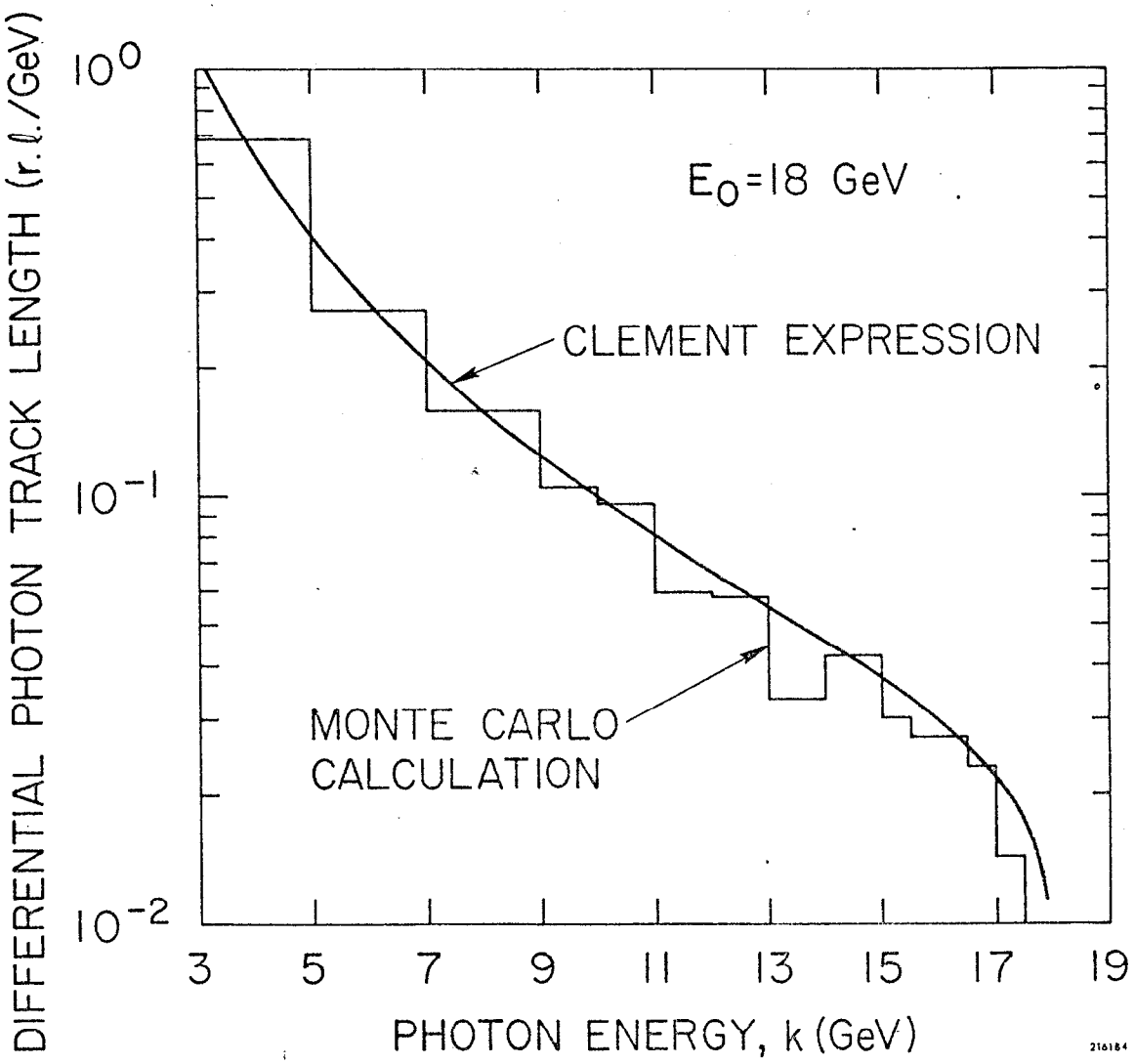
DIFFERENTIAL PHOTON TRACK LENGTH (r.ℓ./GeV)
10^0
10^-1
10^-2
E_0=18 GeV
CLEMENT EXPRESSION
MONTE CARLO
CALCULATION
3
5
7
9
11
13
15
17
19
PHOTON ENERGY, k (GeV)
216184

Fig. 1

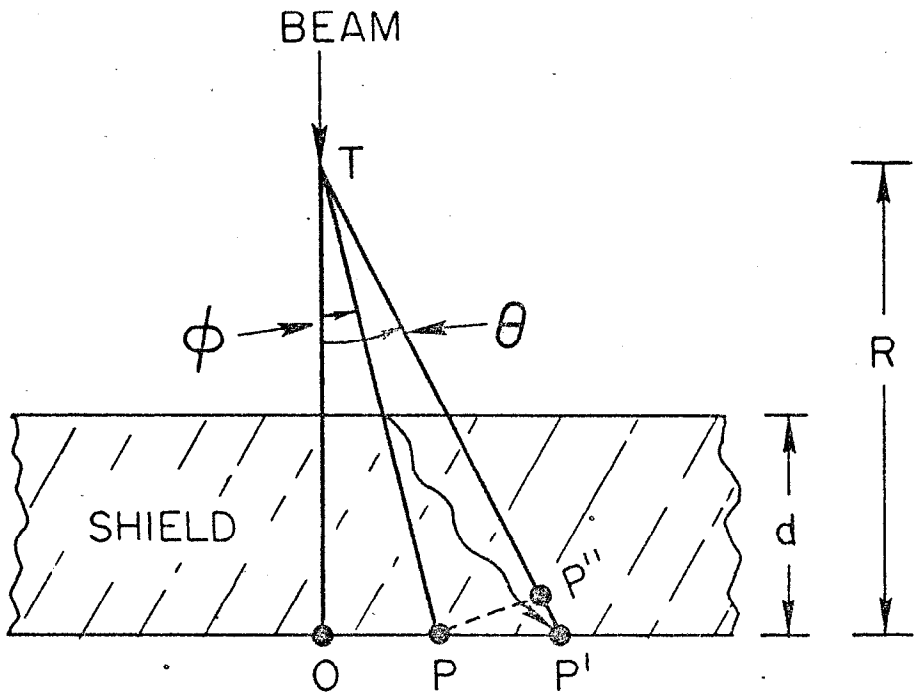

(a)

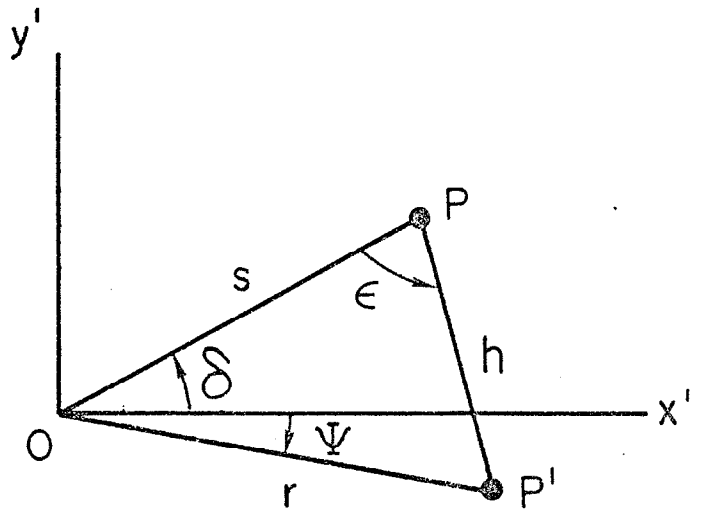

(b)

1130A10

Fig. 2

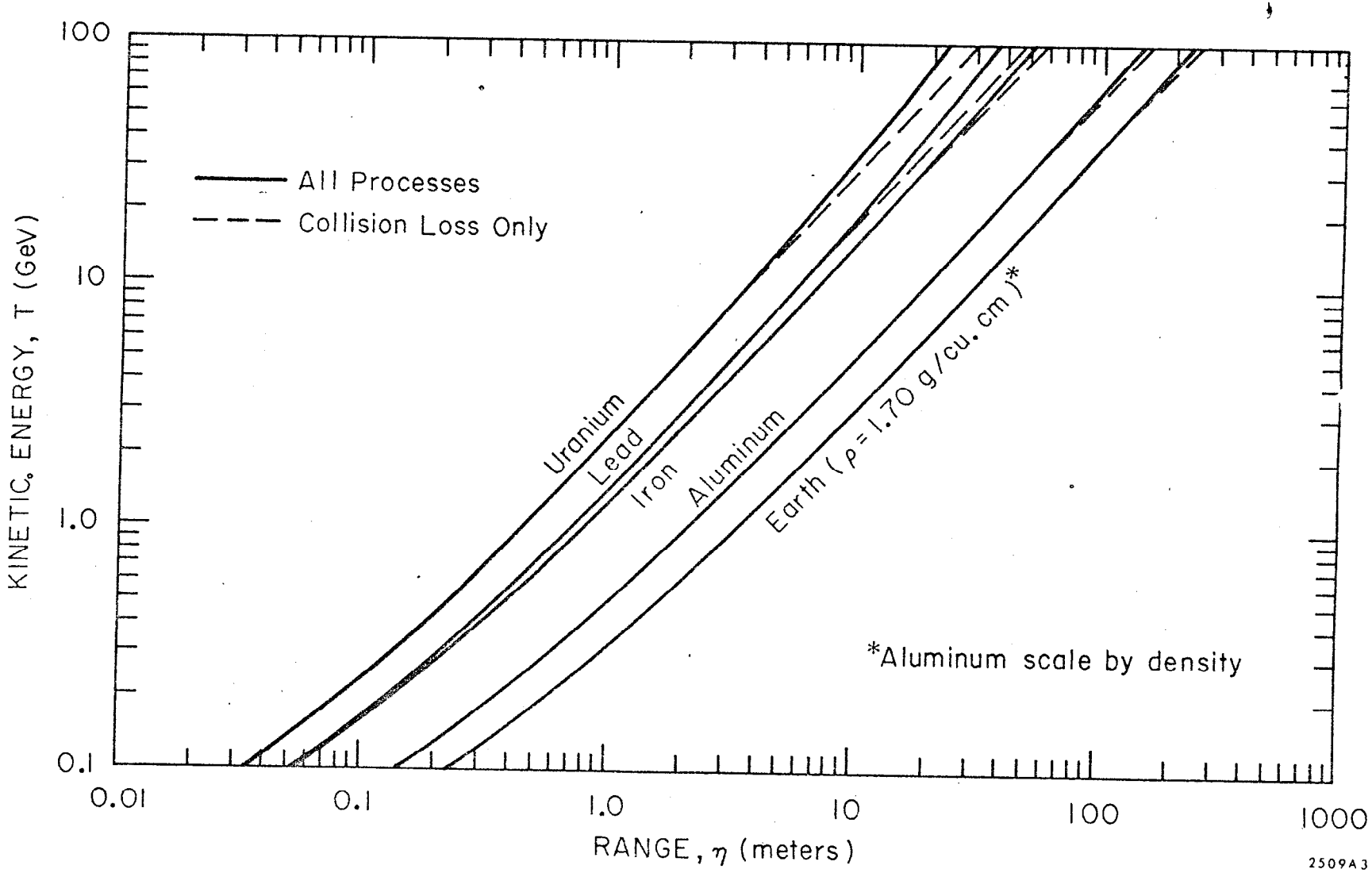
100
10
1.0
0.1
KINETIC ENERGY, T (GeV)
All Processes
Collision Loss Only
Uranium
Lead
Iron
Aluminum
Earth (ρ = 1.70 g/cu. cm)*
*Aluminum scale by density
0.01
0.1
1.0
10
100
1000
RANGE, η (meters)
2509A3

Fig. 3